

Polarized Neutron Diffraction – A Tool for Testing Extinction Models: Application to Yttrium Iron Garnet

BY MICHEL BONNET, ALAIN DELAPALME AND PIERRE BECKER*

DRF/DN Centre d'Etudes Nucléaires, B.P. 85, Centre Tri, F 38041 Grenoble-Cédex, France

AND HARTMUT FUESS†

Institut Laue-Langevin, B.P. 156, F 38042 Grenoble-Cédex, France

(Received 10 February 1976; accepted 7 April 1976)

The Becker–Coppens treatment of extinction is applied to the polarized neutron technique. Analytical expressions for the extinction correction are derived for plate-like crystals. The formalism is applied to data collected on yttrium iron garnet. Measurements were performed on crystals of various thicknesses using wavelengths in the range 0.5–1.1 Å. The correction is shown to be quite adequate even for severe extinction, with a preference for Lorentzian shape of $\bar{\sigma}$, the mean diffracting power, though some systematic deviations are present. The method is shown to be very sensitive to a given model for extinction, mainly because of the independence from any scale factor. It is demonstrated that the flipping ratio R can be out of the range [$R_{\text{kinematic}}$, R_{dynamic}] and that such a situation implies the simultaneous presence of primary and secondary extinction and one can have $R = R_{\text{dynamic}}$ for a crystal far from dynamical behaviour. Application of a recent dynamical test proposed by Kato [*Acta Cryst.* (1976), A32, 453–466] concerning the validity of the physical assumption of the model shows that in neutron refinement for most reflexions the situation is encouraging. Estimation of mosaic spread by γ -ray diffraction leads to a fair agreement with the refined values.

Introduction

There are two approaches to the theory of diffraction in crystals. The dynamical theory is the more general one but can only be applied to crystals that are perfect or show only small distortions. The kinematical theory is the limit of the preceding one in the case of small coherent domains or short wavelengths: it is widely used in structural crystallography.

For most crystals the situation is intermediate between these two extreme cases and extinction models are necessary to obtain the Fourier components of the electronic density. Until now, extinction models have been described starting from the kinematical theory and using the energy transfer equations of Darwin (1922): this 'mosaic model' has been further developed by Hamilton (1957), Zachariasen (1945, 1967), and by Becker & Coppens (1974 – hereafter referred as to BC). Recently Kato (1976) has proposed a first approach to the problem, starting from the Takagi–Taupin equations of dynamical theory, and describing the distortion in terms of an ensemble average. This treatment justifies the use of energy transfer equations under specific conditions.

The purpose of this paper is to show that polarized neutron experiments, which do not depend on any scale factor, are very dependent on extinction and

provide original tests for extinction models. Moon, Koehler, Cable & Child (1972 – hereafter referred as to MKCC) have formulated the problem and proposed a first-order solution applicable only when the extinction is small. In the first part, some analytical derivations of secondary extinction corrections are discussed, using BC formalism (the same notation will be used). In the second part, the main principles governing polarized neutron diffraction are briefly reviewed, with a special discussion of extinction problems. The method is then applied to the case of yttrium iron garnet (YIG). This experiment shows the technique of polarized neutrons to be very powerful for testing extinction models and for deciding whether the crystal behaves dynamically or kinematically (following Kato's criterion).

I. Analytical expressions for secondary extinction

The extinction correction y is defined as the reduction of the integrated intensity P from the kinematical value P_k :

$$P = P_k y. \quad (1)$$

This coefficient consists of a factor $y_p(x_p)$ for primary extinction in the coherent domains and a factor $y_s(y_p x_s)$ for secondary extinction between these domains. The expression used for y is

$$y = y_p(x_p) y_s(y_p x_s). \quad (2)$$

BC gave an approximation to the expression for y , when absorption is negligible,

* Permanent address: Centre de Mécanique Ondulatoire du CNRS, 23 rue du Maroc, 75019 Paris, France.

† Present address: Institut für Kristallographie der Universität, D 6000 Frankfurt/Main, Senckenberg Anlage 30, Germany (BRD).

$$y_s \simeq \sum_{n=0}^{\infty} \frac{(-1)^n}{n!} \overline{T^{(n)}} Q^{-1} \int \bar{\sigma}^{n+1}(\varepsilon_1) d\varepsilon_1 \quad (3a)$$

with

$$\overline{T^{(n)}} = v^{-1} \sum_{j=0}^n \binom{n}{j}^2 \int_v T_1^j T_2^{n-j} dv. \quad (3b)$$

$\bar{\sigma}(\varepsilon_1)$ stands for the mean diffracting power for a given divergence ε_1 of the incident beam from the Bragg condition

$$\bar{\sigma} = \sigma * W, \quad (4)$$

where $\sigma(\varepsilon_1)$ is the diffracting power of an average coherent domain and $W(\varepsilon_1)$ the angular distribution of those domains.

Zachariasen (1967) has pointed out that if the widths of $\sigma(\varepsilon_1)$ and $W(\varepsilon_1)$ are of the same order of magnitude, secondary extinction depends on two parameters, the mean angular misorientation (g) and the size of the mean coherent domain (t). In equations (3), T_1 and T_2 are the respective path lengths along the incident and diffracted directions and the integral in (3b) is taken over the crystal volume v .

It can be shown (Appendix A) that (3) represents the exact solution of the energy transfer equations [BC equation (10)] when the crystal is in a pure Laue case.

The order of magnitude of primary extinction is described by BC with an expression similar to (3).

Equations (3) have been numerically solved by BC for the case of spherical and ellipsoidal crystals, for various shapes of $W(\varepsilon_1)$. In neutron diffraction, the choice of a plate-like crystal is often preferable to get enough diffracted intensity and reasonable extinction. We shall concentrate here on such cases.

In Appendix B, a method of calculation of the quantity $\overline{T^{(n)}}$ is described for geometries varying between pure Laue and pure Bragg. In the Laue case it is shown that

$$\begin{aligned} \overline{T^{(n)}} &= \frac{a^n}{n+1} \left[\frac{1}{\cos \alpha_1} + \frac{1}{(\cos \alpha_2)C} \right]^n - \frac{na^{n+1}}{b(n+1)(n+2)} \\ &\times \left[\frac{1}{\cos \alpha_1} + \frac{1}{(\cos \alpha_2)C} \right]^{n-1} \\ &\times \left(\frac{\tan \alpha_1}{\cos \alpha_1} + \frac{\tan \alpha_2}{(\cos \alpha_2)C} \right). \end{aligned} \quad (5)$$

In this expression, a is the thickness of the plate, b the width of the entrance face, α_1 and α_2 the angles between the normal to the plate and the incident and diffracted beams. $C=1$ in equatorial conditions and can be approximated to $\cos \mu_2$ when the angle μ_2 between the diffracted beam and the equatorial plane is small.

In other cases, the approximation is less simple and it is always possible to use the approximation of a large plate (b/a large) so that (5) reduces to

$$\overline{T^{(n)}} \sim \frac{2^n}{n+1} [\overline{T^{(1)}}]^n \quad (6)$$

where $\overline{T^{(1)}}$, the actual value for a finite crystal, can be obtained exactly.

Expressions for the extinction correction y are also derived in Appendix B for both a Lorentzian and a Gaussian distribution $\bar{\sigma}(\varepsilon_1)$ and it is shown that in some cases the series expansion reduces to a closed form.

II. Extinction in polarized neutron diffraction

Neutrons are two-spin-state particles and polarized neutron beams are composed of neutrons in only one spin state. Collecting the intensities P^+ and P^- for up and down spin states yields the 'flipping ratio',

$$R = \frac{P^+}{P^-}, \quad (7)$$

which does not depend on any scale factor. The following experimental conditions are assumed to be realized: (a) no half-wavelength contamination, (b) perfectly polarized incident beam, (c) the magnetic moments are all aligned with the neutron spins. We shall call ω the angle between the direction of magnetization and the diffusion vector and define $q^2 = \sin^2 \omega$.

II. 1. Kinematical case

Using an ideally imperfect crystal (or a powder) and choosing ($q^2=1$), the value of the flipping ratio is given by

$$R = R_K = \left[\frac{F_N + F_M}{F_N - F_M} \right]^2. \quad (8)$$

F_N , the nuclear structure factor, is given by the well known formula

$$F_N = \sum_j b_j \exp(2\pi i \mathbf{H} \cdot \mathbf{r}_j) \exp(-W_j);$$

and F_M , the magnetic structure factor, by

$$F_M = \frac{e^2}{2mc^2} \gamma_N \sum_j \mu_j f_j(\mathbf{H}) \exp(2\pi i \mathbf{H} \cdot \mathbf{r}_j) \exp(-W_j),$$

where μ_j is the algebraic value of the magnetic moment, in Bohr magnetons, of the site j and $f_j(\mathbf{H})$ is the normalized magnetic form factor of this site, γ_N is the moment of a neutron in nuclear magnetons.

II. 2. Dynamical case

Under the same experimental conditions but using a perfect thick crystal

$$R = R_D = \left(\frac{F_N + F_M}{F_N - F_M} \right) = R_K^{1/2}. \quad (9)$$

The dynamical flipping ratio R_D can be derived from the kinematical value, which can be determined experimentally by applying the polarized neutron technique to fine magnetically aligned powders.

II. 3. Practical case of a real crystal

MKCC give in their equation (A1) generalized energy transfer equations for polarized neutron diffraction, which can be written with BC notation

$$\begin{aligned}\frac{\partial I_0^+}{\partial x_1} &= -\bar{\sigma}^+ I_0^+ + \bar{\sigma}^{++} I^+ + \bar{\sigma}^{-+} I^- \\ \frac{\partial I^+}{\partial x_2} &= -\bar{\sigma}^+ I^+ + \bar{\sigma}^{++} I_0^+ + \bar{\sigma}^{-+} I_0^- \\ \frac{\partial I_0^-}{\partial x_1} &= -\bar{\sigma}^- I_0^- + \bar{\sigma}^{--} I^- + \bar{\sigma}^{+-} I^+ \\ \frac{\partial I^-}{\partial x_2} &= -\bar{\sigma}^- I^- + \bar{\sigma}^{--} I_0^- + \bar{\sigma}^{+-} I_0^+.\end{aligned}\quad (10)$$

Equations (10) do not take into account absorption and depolarization: these effects would, for example, add a term $(-\mu_d I_0^+ + \mu_d I_0^- - \mu_d I_0^+)$ to the first equation and so on for the others, if μ_d and μ_a are respectively the coefficients of depolarization and absorption. I_0^\pm and I^\pm refer to incident and diffracted intensities, + and - to the spin state of the neutrons.

$\bar{\sigma}^{ij}(\varepsilon_1)$ is the diffracting power for an incident neutron in spin state i diffracted in spin state j . $\bar{\sigma}^+(\varepsilon_1)$ and $\bar{\sigma}^-(\varepsilon_1)$ are defined as

$$\begin{aligned}\bar{\sigma}^+ &= \bar{\sigma}^{++} + \bar{\sigma}^{+-} \\ \bar{\sigma}^- &= \bar{\sigma}^{--} + \bar{\sigma}^{-+}\end{aligned}\quad (11)$$

and represent the total diffracting power for incident neutrons in a given spin state. The diffracting powers $\sigma^{ij}(\varepsilon_1)$, which are defined as in BC treatment, differ from one another by $|F^{ij}|^2$:

$$\begin{aligned}\bar{\sigma}^{++}(\varepsilon_1) &= \chi(\varepsilon_1) |F^{++}|^2 = \chi(\varepsilon_1) |F_N + q^2 F_M|^2 \\ \bar{\sigma}^{--}(\varepsilon_1) &= \chi(\varepsilon_1) |F^{--}|^2 = \chi(\varepsilon_1) |F_N - q^2 F_M|^2 \\ \bar{\sigma}^{+-}(\varepsilon_1) &= \bar{\sigma}^{-+}(\varepsilon_1) = \chi(\varepsilon_1) |F^{+-}|^2 = \chi(\varepsilon_1) |F_M|^2 q^2 (1 - q^2).\end{aligned}\quad (12)$$

$\chi(\varepsilon_1)$ is a Lorentzian or Gaussian function of ε_1 .

The spin flip diffracting power $\sigma^{+-}(\varepsilon_1)$ is generally very small since $|F_M|$ is small and q^2 is often equal to 1. With the assumption that $\bar{\sigma}^{+-} = 0$, the system (10) reduces to equations equivalent to the system BC equation (10) for the appropriate polarization state and can be solved as discussed in § I.

When necessary one may estimate the perturbing effect of $\bar{\sigma}^{+-}$ by a first and second-order correction, as discussed by MKCC. If for a given reflexion, this correction is of significant value, one should be cautious in the interpretation of this reflexion, unless a better solution of the system (10) can be found.

With these assumptions, the actual value of the flipping ratio can be written

$$R = R_K \frac{y^+}{y^-}\quad (13)$$

where y^\pm obey equations (2) and refer to σ^\pm (equation 11). In the following we have omitted the \pm signs.

The secondary extinction coefficient y_s (3) is given by

$$y_s = \sum_{n=0}^{\infty} \left(-\frac{Q\alpha_L y_p}{3} \right)^n \binom{2n}{n} \frac{\overline{T^{(n)}}}{n!}\quad (14)$$

for a Lorentzian distribution, and by

$$y_s = \sum_{n=0}^{\infty} (-Q\alpha_G y_p)^n \frac{\overline{T^{(n)}}}{n! \sqrt{(n+1)}}\quad (15)$$

for a Gaussian distribution, with

$$\alpha_L = \left(\frac{\lambda}{t \sin 2\theta} + \frac{2}{3g} \right)^{-1}\quad (16)$$

$$\alpha_G = \left[\left(\frac{\lambda}{t \sin 2\theta} \right)^2 + \frac{1}{2g^2} \right]^{-1/2}.\quad (17)$$

The small coherent domains are assumed to be isotropically distributed and the primary extinction y_p can be estimated [BC equation (37)] as

$$y_p = \left[1 + 2x_p + \frac{A(\theta)x_p^2}{1 + B(\theta)x_p} \right]^{-1/2}\quad (18)$$

with

$$x_p = \frac{2}{3} Q \frac{\sin 2\theta}{\lambda} t^2.\quad (19)$$

The dynamical theory of diffraction may, in some simple cases, provide an answer to the problem of primary extinction. Unfortunately, the shape of the coherent domains changes drastically within the crystal and a statistical expression for y_p is completely unknown. Therefore, it is not obvious whether, provided y_p is not too small ($y_p > 0.7$), its description by a formula like (18) is unreasonable; and the present treatment of small primary extinction has the advantage of internal consistency.

III. Study of extinction on yttrium iron garnet (YIG)

The flipping ratio R has been measured for about 250 reflexions of YIG (Bonnet, Delapalme, Tch  ou & Fuess, 1974). The reflexions suffering highly from extinction were measured on different plate-shaped crystals: YIG-1 ($5 \times 2.7 \times 1$ mm), YIG-2 ($4 \times 2.7 \times 0.3$ mm), YIG-3 ($4 \times 1.7 \times 0.8$ mm), YIG-4 ($4 \times 2.7 \times 1$ mm). The dimensions are along the directions [111], [110], [112], respectively. All structural information has been discussed by Bonnet, Delapalme, Fuess & Thomas (1975). Measurements were performed with the goniometer DN2 at Melusine (CENG) and the D5 facility of the high flux reactor at ILL, both in Grenoble (this last instrument is installed at a hot source and allows measurements at wavelength down to 0.5  ). Several reflexions were observed on the different samples, at various wavelengths. YIG-4 was studied more extensively, then reduced in thickness to 0.3 mm and the measurements were repeated. Moreover, powder measurements were done with both polarized and unpolarized neutrons on a sample in which the magnetic

moments were aligned with the magnetic field. For equatorial reflexions, these measurements yield the kinematical flipping ratio R_K [equation (8)], from which the dynamical R_D is derived.

III. 1. Methods of refinement

In a first refinement, we have minimized for each sample the quantity

$$\varphi = \sum_j w_j \left(R_j - R_{iK} \frac{y_j^+}{y_j^-} \right)^2 \quad (20)$$

with respect to t , g and R_K : from R_K , since the crystal is centrosymmetric and F_N is known (Bonnet *et al.*, 1975) one can derive F_M and therefore calculate y^+ and y^- . In the summation (20), all the independent measurements relative to a given sample are included (e.g., in the case of YIG-4, 51 observations were used, corresponding to 12 reflexions). w_i was chosen as

$$\frac{1}{w_i} = \sigma^2(R_i) = \sigma_c^2(R_i) + (k_w R_K e_i)^2 \quad (21)$$

where e_i is defined as

$$e_i = 1 - \frac{y_i^+}{y_i^-}. \quad (22)$$

In (21) σ_c^2 comes from counting statistics, and k_w is adjusted so that the standard deviation of the observation of unit weight S is closest to 1.

$$S = \frac{1}{n_o - n_v} \sum_i w_i \left(R_i - R_{iK} \frac{y_i^+}{y_i^-} \right). \quad (23)$$

n_o and n_v are respectively the number of observations and the number of adjusted parameters. The weighted agreement index is defined as

$$R_w(R) = \left(\frac{\varphi}{\sum_i w_i R_i^2} \right)^{1/2}. \quad (24)$$

The refinements were done for Lorentzian and Gaussian distributions and the results for YIG-4 are shown on Table 1. For the same sample φ was calculated as a function of t and η and was plotted in Fig. 1. It is clear that the refinement converges towards a unique minimum and in a region far away from the one where primary extinction is predominant.

In a second procedure the refinements were carried out on the magnetic structure factor, like in a conventional X-ray refinement. The advantage of this proce-

dure is the possibility of refining directly on the magnetic form factor. In the same refinement, we have simultaneously introduced all the R_{obs} corresponding to YIG-1 and YIG-4 (before and after reduction of the thickness) for the various wavelengths (in the range 0.5–1.1 Å). The nuclear positions and Debye–Waller factors were kept constant and different adjustable extinction parameters t and g were introduced for YIG-1 and YIG-4. Since the extinction factor y^+/y^- differs from 1 by a term proportional to $(F_N F_M)$ to a first approximation, the variance σ^2 for each observation was taken as

$$\sigma^2(F_M) = \sigma_c^2(F_M) + k_w' \frac{F_M F_N \lambda^3}{\sin 2\theta} \overline{T^{(1)}}. \quad (25)$$

The results are shown in Table 2 and, compared with those of Table 1, show a close agreement for t and g within their standard deviation.

It may be pointed out that an X-ray refinement from a sphere of YIG (Bonnet *et al.*, 1975) yielded extinction parameters $t = 7 \mu\text{m}$, $g = 5 \times 10^4$, which are of the same order of magnitude as those of Table 1.

III. 2. Discussion of the results

The best fit is obtained for the hypothesis of a Lorentzian diffracting power $\bar{\sigma}(\epsilon_1)$.

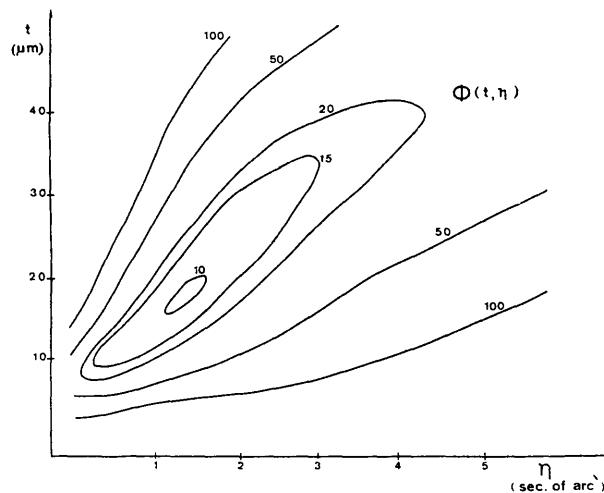


Fig. 1. Map of the function φ minimized by least squares as a function of the extinction parameters t and η for a Lorentzian distribution.

Table 1. Refined extinctions parameters t , g and agreement factors on flipping ratio R for YIG-4

	Distribution of coherent domains			Agreement factors		
	Size t (μm)	Disorientation $g \times 10^{-4}$	η (s of arc)	R (R)	R_w (R)	S
Gaussian	9.62 (2.0)	2.36 (0.4)	2.46	0.0152	0.0161	2.08
Lorentzian	16.98 (3.0)	4.24 (0.8)	1.37	0.0118	0.0118	1.11

(a) Let us consider the reflexion $6\bar{4}2$. In Fig. 2(a), the flipping ratio R_{obs} is plotted versus the quantity $[\xi = \lambda^3 \bar{T}^{(1)} / \sin 2\theta]$. The experimental points are displayed mostly between R_K and R_D (R_K is obtained from the powder experiment). Fig. 2(b) shows the magnitude of F_M as a function of the same parameter (ξ). The upper (open stars) and lower (shaded stars) results represent values of F_M calculated from R_D and R_K respectively. The actual values (shaded squares) are obtained by applying the extinction correction discussed in § II. It can be concluded that even the most severely extinction-affected points lie within one standard deviation of the horizontal line obtained from the powder measurement. It seems that the crystal tends towards dynamical behaviour for the highest values of ξ . Let us investigate this point further, using the measurement on a very thick crystal (~ 12 mm).

With this crystal, R values have been observed that are significantly out of the range (R_K, R_D) (Table 3): $R > R_D$ if $R_K < 1$, $R < R_D$ if $R_K > 1$. The question is therefore the following: does the fact that R is equal to or beyond R_D imply that we are in a dynamical situation (only primary extinction). For severe extinction BC have shown that $y_s(x)$ behaves like $x_s^{-1/2}$. Therefore from equation (2)

$$y \propto y_p \frac{1}{|F|/y_p} = \frac{y_p}{F}$$

so that

$$P \propto F/y_p. \tag{26}$$

It is well known that in the upper limit of primary extinction y_p varies as $1/F$. Therefore P will vary as F^m , m being in the range $[\frac{1}{2}, 2]$ and for polarized neutrons, $R(\sim R_D^m)$ will be in the range $[R_K, R_D^{1/2}]$. In conclusion, if the crystal behaves dynamically $R = R_D$ but the converse may not be true. The values of m for the three reflexions of Table 3 agree with this discussion, and it should be noticed that these reflexions are listed in terms of decreasing extinction. This discussion should without doubt give confidence in the behaviour of y proposed by BC [equation (2)].

Table 3. Observed compared with the kinematical and dynamical flipping ratios for a thick crystal (~ 12 mm)

<i>hkl</i>	R_{obs}	R_D	R_K	m
$2\bar{2}0$	0.787 (3)	0.636	0.405	0.529
$6\bar{4}2$	0.850 (3)	0.778	0.608	0.647
440	4.17 (2)	4.49	20.2	0.95

Table 2. Refined extinction parameters t , g and agreement factors on magnetic structure factor F_M for YIG-1 and YIG-4

	YIG-1		YIG-4		All reflexions			0.83 > y^+/y^- > 1.20		
	t (μm)	$g \times 10^{-4}$	t (μm)	$g \times 10^{-4}$	R (F)	R_w (F)	S	R (F)	R_w (F)	S
Lorentzian	19.8 (4.2)	2.1 (0.4)	14.9 (3.0)	4.0 (1.0)	0.0365	0.0388	1.20	0.0283	0.0325	1.49
Gaussian	9.9 (5.2)	1.1 (0.1)	15.2 (3.6)	1.6 (0.2)	0.0493	0.0433	1.47	0.0424	0.0449	3.28

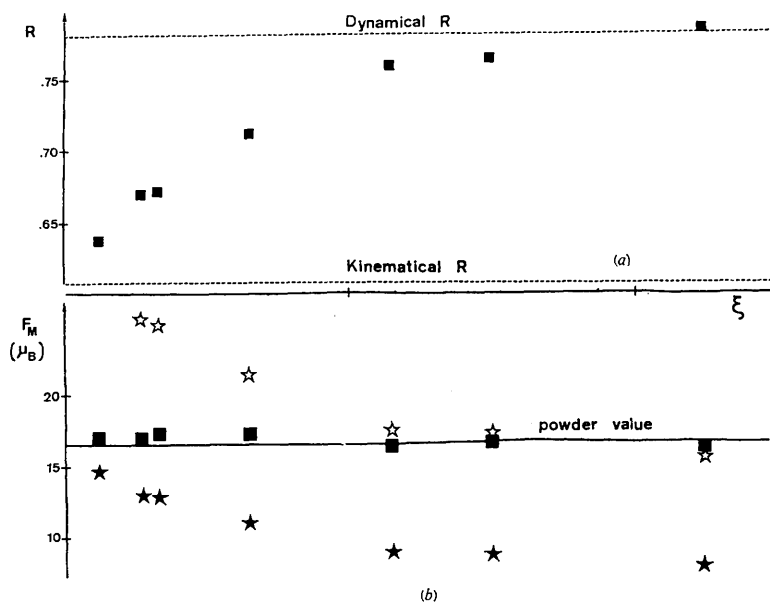


Fig. 2. (a) Flipping ratio of the $6\bar{4}2$ reflexion as a function of ξ (wavelength and thickness). (b) Magnetic structure factor F_M as a function of ξ . Extinction corrected \blacksquare , kinematical \star and dynamical \star values.

(b) With the definition of e (22) one can write

$$R = R_K(1 - e). \quad (27)$$

If R_K is known from a powder measurement, it is possible to draw the straight line (27) as a function of $|e|$ ($e > 0$ if $y^+/y^- < 1$, $e < 0$ if $y^+/y^- > 1$). This was done in Fig. 3(a) and (b) for the two reflexions $2\bar{2}0$ and $6\bar{4}2$: in this figure, the measured values of R , for the four samples, different wavelengths and thickness have been plotted as a function of $|e|$ calculated from the refined values of t and g and assuming a Lorentzian distribution (t and g depend on the sample to which is referred). The quality of the model used for extinction can be appreciated by the departure of the points from the 'theoretical' line (27). In this practical case, the fact that the points corresponding to different samples and different wavelengths are homogeneously aligned show the type of correction to be quite general.

(c) In Fig. 4, the values of R as function of $|e|$ are plotted for the reflexion $2\bar{2}0$ (crystal YIG-4) assuming either a Lorentzian or a Gaussian distribution. It appears that for large values of $|e|$, the Lorentzian correction slightly undercorrects, while the Gaussian correction strongly overcorrects for extinction. The same effect was observed for many reflexions. The method of polarized neutrons seems therefore to be sensitive to the type of statistical distribution used to describe the defects of the sample.

(d) The same conclusion can be drawn from Table 4 in which the magnetic structure factors of the $6\bar{4}2$ reflexion, corrected for extinction, are reported. The extinction factors are given in order to show the relative influence of primary and secondary extinction.

(e) In order to check for the significance of the refined parameter g , the mosaic spread η ($\eta = 1/2/\pi g$) has been estimated by the gamma-ray diffraction technique (Schneider, 1974) on the crystal YIG-1. We have chosen the reflexion $6\bar{4}2$ for which mosaic spread is the dominant factor governing its extinction. The width of the measured rocking curve is about $17''$ but

the resolution of the apparatus is $10''$. Therefore it is necessary to deconvolute from the instrumental width and, depending on the assumed shape of the rocking curve, one obtains

$$\eta_{\text{obs}} \in [3'', 6''] .$$

The calculated value of η (from Table 2) is found to be $6''$ for a Gaussian $\bar{\sigma}$ and $3''$ for a Lorentzian $\bar{\sigma}$.

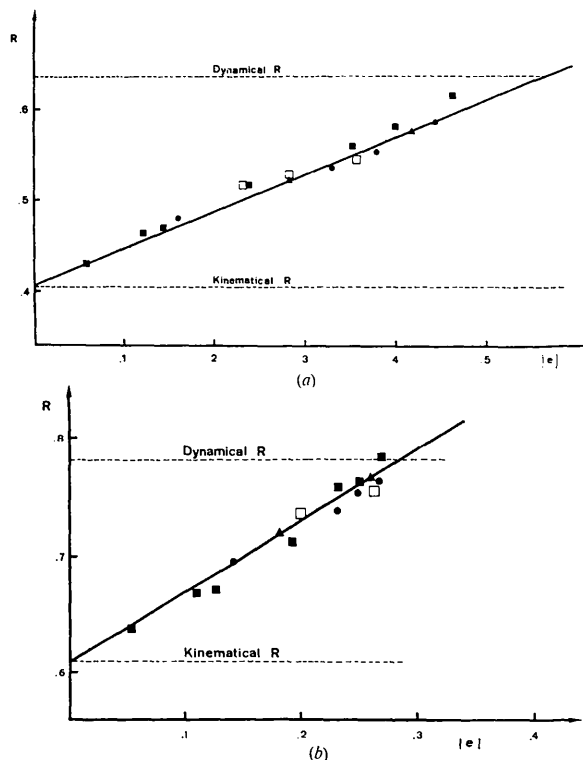


Fig. 3. Measured flipping ratio R as function of $|e|$ with a Lorentzian extinction correction for YIG-1 ●, YIG-2 □, YIG-3 ▲ and YIG-4 ■. Comparison with the straight line (27) for (a) $2\bar{2}0$ and (b) $6\bar{4}2$ reflexions.

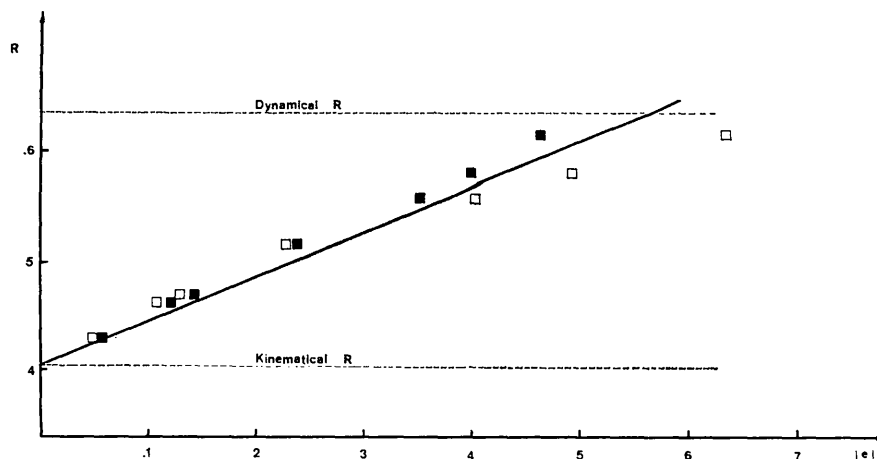


Fig. 4. Measured flipping ratio R as function of $|e|$ for Lorentzian ■ and Gaussian □ extinction correction. Comparison with the straight line (27) (YIG-4 $2\bar{2}0$).

Repeated measurements changing the setting angles and for a few other reflexions lead to the same values and do not reveal any significant anisotropy of the mosaic distribution. Therefore the refined value of g is of some physical significance.

(f) Finally we want to test the validity of the model of energy transfer equations in terms of the condition introduced by Kato (1976). He introduces a correlation length τ_2 which can be shown to vary between a coherence length (which can be compared to t) and a misorientation length (to be compared to $g\lambda/\sin 2\theta$). The condition can be expressed as:

$$\tau_2 \ll A \sim \frac{V}{2\lambda|F^{ij}|}. \quad (28)$$

V is the unit-cell volume and the smallest value of A in this case is $\sim 25\mu$. For YIG-4 the refined extinction parameters are $t \sim 15\mu$, $t^* = g\lambda/\sin 2\theta \sim 5/\sin 2\theta$.

For the smallest Bragg angle $t^* \sim 22\mu$. In such a situation the condition (28) is not exactly fulfilled. The situation improves when $\sin 2\theta$ increases since, at the same time, the influence of 'particle size effect' decreases. Therefore, though for some small-angle reflexions the basic assumptions of the 'incoherent' description of extinction are not well satisfied, the model seems to give satisfactory correction and its domain of validity (as shown also by most of the cases discussed in the literature) may be less strict than (28). It should be noticed that in most of the neutron diffraction experiments, the situation should be less dramatic.

The authors are indebted to Dr J. Schneider for helping in the γ -ray measurements. They also thank Professor N. Kato for his interest in the experi-

mental tests for extinction and for helpful discussion, and the other members of the polarized neutron group, Drs J. Schweizer, F. Tasset and J. X. Boucherle, for stimulating and valuable discussions. We are grateful to Professor E. F. Bertaut for encouraging this work.

APPENDIX A

On the accuracy of the solution (3) of Becker & Coppens (1974)

The section of a general, convex-shaped crystal in a plane parallel to the incident direction (unit vector \mathbf{u}_0^0) and the diffracted direction (unit vector \mathbf{u}^0) is represented on Fig. 5. The entrance surface is $A_1B_1A_2$ and the exit surface is $B_1A_2B_2$. There is an overlap region B_1A_2 . Becker & Coppens (1974) (BC) have shown that the extinction correction can be formally calculated by an iterative procedure. Each step of the calculation involves integration of a volume associated with each current point M , and is shown in Fig. 6: the two possible situations as shown in Fig. 6(a) and (b) depend on the position of M with respect to B_1 . $T_1(M)$ is the depth along the incident direction: $T_1(M) = M_1^0M$. The integrand involves the quantity $\min [T_1(M), T_1(M_1)]$. The assumption made by BC is to replace this quantity by $T_1(M_1)$ and it leads to the solution (3) without any further approximation.

(a) If M_1^0 is between A_1 and B_1 (Laue case)
 $\min [T_1(M), T_1(M_1)] = T_1(M_1)$.

(b) If M_1^0 is between B_1 and A_2 (Bragg case), the situation is more complex;

If $M_1 \in |Q, M|$: $\min [T_1(M), T_1(M_1)] = T_1(M)$,

If $M_1 \in |M_1^0, Q|$: $\min [T_1(M), T_1(M_1)] = T_1(M_1)$.

Table 4. Results for YIG-4 $6\bar{4}2$ reflexion; flipping ratio, corrected magnetic structure factor, primary and secondary extinction factor for each spin state, as functions of thickness and wavelength

t (mm)		Quantities in parentheses are standard deviations.						
λ (Å)	R	F_M Gauss	F_M Lorentz	y_P^+	y_P^-	y_S^+	y_S^-	y^+/y^-
1.00	0.784	18.24	16.13	0.96	0.94	0.45	0.36	1.27
1.10	(0.004)	(0.8)	(0.8)					
1.00	0.762	17.54	16.57	0.97	0.96	0.53	0.43	1.25
0.92	(0.003)	(0.7)	(0.7)					
1.00	0.759	16.51	16.25	0.98	0.97	0.58	0.48	1.23
0.812	(0.003)	(0.6)	(0.6)					
0.3	0.711	16.62	17.27	0.96	0.94	0.71	0.61	1.19
1.10	(0.004)	(0.5)	(0.5)					
0.3	0.671	16.43	17.30	0.98	0.97	0.82	0.73	1.13
0.812	(0.003)	(0.4)	(0.4)					
0.3	0.669	16.07	16.91	0.98	0.97	0.84	0.77	1.11
0.74	(0.003)	(0.4)	(0.4)					
0.3	0.637	16.32	16.84	0.99	0.99	0.92	0.88	1.06
0.5	(0.003)	(0.3)	(0.3)					
powder	0.608	16.65	16.65	1	1	1	1	1
1.104	(0.005)	(0.4)	(0.4)					

BC have shown that (3) is exact if $\theta=0$, and that the solution is valid to the third order in x for $2\theta=\pi$.

This discussion shows that the approximation comes from the mixture of Laue and Bragg geometry. Many crystals, particularly in neutron diffraction, have simple shapes, e.g. parallelepipeds and plates. Such a situation is represented in Fig. 7, for a parallelepiped. There are two situations for which no overlap occurs between the entrance and exit surface; the incident and diffracted directions must lie in opposite quadrants.

Many reflexions satisfy the condition of a pure Laue case, for which the solution (3) is exact. When the number of limiting planes of the crystal increases, the probability of having a pure Laue case decreases and the limit is a continuous surface, as shown in Fig. 5. The problem of Laue-Bragg cases will be further discussed (Becker, 1976).

APPENDIX B

Analytical expressions for y in Laue geometry

We shall restrict ourselves to the case of plate-like crystals in Laue geometries. The more general case will be discussed later (Becker, 1976).

(1) Let us start with an infinite plate (Fig. 8) and an equatorial reflexion. Let $\gamma_1 = \cos \alpha_1$, $\gamma_2 = \cos \alpha_2$. For the two situations shown in Fig. 8(a) and (b), the values of $\overline{T^{(n)}}$ and of the extinction correction will be the same. (a) $\alpha_2 - \alpha_1 = 2\theta$, (b) $\alpha_1 + \alpha_2 = 2\theta$.

Let x be the coordinate perpendicular to the crystal, $x \in [0, a]$, $T_1 = x/\gamma_1$, $T_2 = (a-x)/\gamma_2$. From (3)

$$\overline{T^{(n)}} = a^{-1} \sum_{j=0}^{\infty} \binom{n}{j}^2 \frac{1}{\gamma_1^{n-j}} \frac{1}{\gamma_2^j} \int_0^a x^{n-j} (a-x)^j dx;$$

since

$$\int_0^a x^p (a-x)^q dx = \frac{a^{p+q+1}}{(p+q+1) \binom{p+q}{q}}$$

one obtains

$$\overline{T^{(n)}} = \frac{1}{n+1} \left(\frac{a}{\gamma_1} + \frac{a}{\gamma_2} \right)^n = \frac{[2\overline{T^{(1)}}]^n}{n+1}. \tag{B1}$$

This relation is similar to (6).

If the beams do not lie in the equatorial plan, (B1) should remain the same, provided $\overline{T^{(1)}}$ is changed to

$$\overline{T^{(1)}} = a \left[\frac{1}{\gamma_1 \cos \mu_1} + \frac{1}{\gamma_2 \cos \mu_2} \right],$$

where μ_1 and μ_2 are the angles of the incident and diffracted beams with the equatorial plan.

Suppose the distribution function $\overline{\sigma(\epsilon_1)}$ to be Lorentzian. Using equation (14), one obtains

$$\begin{aligned} y_s &= \sum_{n=0}^{\infty} \left(\frac{-2Q\alpha_L y_p}{3} \right)^n \binom{2n}{n} \frac{[\overline{T^{(1)}}]^n}{(n+1)!} \\ &= \sum_{n=0}^{\infty} (-y_p x_s)^n \binom{2n}{n} \frac{1}{(n+1)!}. \end{aligned}$$

We define z as

$$z = y_p x_s$$

and use the identity

$$\exp(-u) I_0(u) = \sum_0^{\infty} (-1)^n \left(\frac{u}{2} \right)^n \frac{1}{n!}.$$

Therefore,

$$y_s(z) = \frac{1}{z} \int \exp(-2z) I_0(2z) dz$$

and the final expression uses the Bessel functions I_0 and I_1 :

$$y_s(z) = \exp(-2z) [I_0(2z) + I_1(2z)]. \tag{B2}$$

In the case of a Gaussian shape for $\overline{\sigma(\epsilon_1)}$, no closed form can easily be found and the series expansion (15) should be employed.

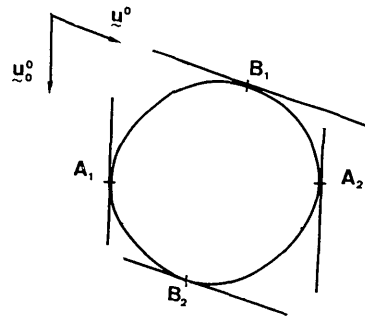


Fig. 5. Section of crystal in a plane parallel to u_0^0 and u_0^0 , the incident and diffracted directions.

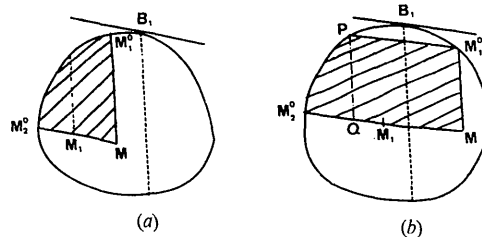


Fig. 6. The two geometrical situations for a point M in the crystal.

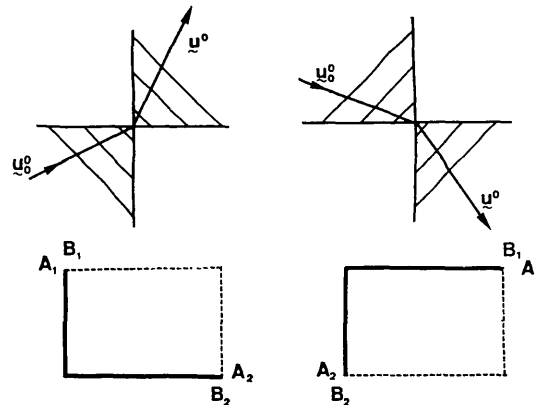


Fig. 7. The Laue case for a parallelepiped-shaped crystal. The full and dashed lines represent the entrance and exit surfaces respectively.

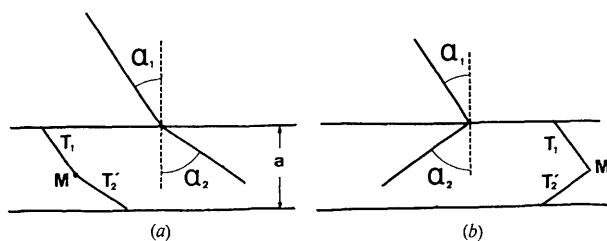


Fig. 8. Case of an infinite plate.

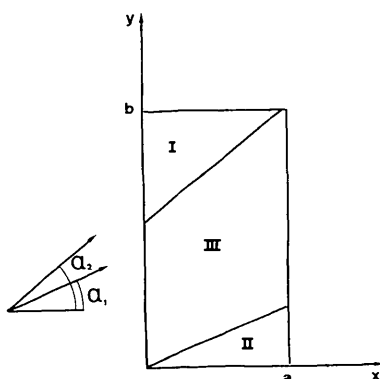


Fig. 9. Case of a finite rectangular plate.

(2) We consider now the Laue case for a finite plate, which is assumed to be rectangular. We assume an equatorial reflexion first (Fig. 9).

The crystal is divided in three parts:

$$\begin{aligned}
 \text{(I)} \quad & x \in [0, a] & y \in [b - (a - x) \tan \alpha_2, b] \\
 & T_1 = \frac{x}{\gamma_1} & T_2' = \frac{b - y}{\gamma_2}, \\
 \text{(II)} \quad & x \in [0, a] & y \in [0, x \tan \alpha_1] \\
 & T_1 = \frac{y}{\gamma_1} & T_2' = \frac{a - x}{\gamma_2}, \\
 \text{(III)} \quad & x \in [0, a] & y \in [x \tan \alpha_1, b - (a - x) \tan \alpha_2] \\
 & T_1 = \frac{x}{\gamma_1} & T_2' = \frac{a - x}{\gamma_2}.
 \end{aligned}$$

By evaluation of the contribution of each domain to the integral for $\overline{T^{(n)}}$, one obtains

$$\begin{aligned}
 \overline{T^{(n)}} = & \frac{a^n}{n+1} \left(\frac{1}{\gamma_1} + \frac{1}{\gamma_2} \right)^n - a^n \frac{a}{b} \frac{n}{(n+1)(n+2)} \\
 & \times \left(\frac{1}{\gamma_1} + \frac{1}{\gamma_2} \right)^{n-1} \left(\frac{\tan \alpha_1}{\gamma_1} + \frac{\tan \alpha_2}{\gamma_2} \right) \quad (B3)
 \end{aligned}$$

where the first term corresponds to the case $a/b \rightarrow 0$ of the infinite plate.

For a Gaussian shape of $\bar{\sigma}$, the series expansion should be used but if $\bar{\sigma}$ is Lorentzian, y_s can be obtained in a closed form. The first term in (B3) will lead to an expression similar to (B2) and from the identity

$$\frac{n}{(n+1)(n+2)} = \frac{1}{n+1} - \frac{2}{(n+1)(n+2)},$$

the contribution of the second term can be also reduced. If we define

$$z = \frac{1}{2} Q \alpha_L y_p a \left[\frac{1}{\gamma_1} + \frac{1}{\gamma_2} \right],$$

then

$$\begin{aligned}
 y_s(z) = & \left[1 + \frac{a \left(\frac{\tan \alpha_1}{\gamma_1} + \frac{\tan \alpha_2}{\gamma_2} \right)}{b \left(\frac{1}{\gamma_1} + \frac{1}{\gamma_2} \right)} \right] \\
 & \times \exp(-2z) [I_0(2z) + I_1(2z)] \\
 & + \frac{a \left(\frac{\tan \alpha_1}{\gamma_1} + \frac{\tan \alpha_2}{\gamma_2} \right)}{b \left(\frac{1}{\gamma_1} + \frac{1}{\gamma_2} \right)} \frac{\exp(-2z)}{z} [I_0(2z) - 1]. \quad (B4)
 \end{aligned}$$

In the case of a non-equatorial reflexion, if the height of the crystal is large, the same result should be obtained, replacing γ_1 by $\gamma_1 \cos \mu_1$ and γ_2 by $\gamma_2 \cos \mu_2$.

References

- BECKER, P. (1976). *Acta Cryst.* To be published.
 BECKER, P. & COPPENS, P. (1974). *Acta Cryst.* A30, 129-153.
 BONNET, M., DELAPALME, A., FUESS, H. & THOMAS, M. (1975). *Acta Cryst.* B31, 2233-2240.
 BONNET, M., DELAPALME, A., TCHÉOU, F. & FUESS, H. (1974). *Int. Congr. Magnetism, Moscow 1973*, Vol. IV, pp. 251-256.
 DARWIN, C. G. (1922). *Phil. Mag.* 43, 800-829.
 HAMILTON, W. C. (1957). *Acta Cryst.* 10, 629-634.
 KATO, N. (1976). *Acta Cryst.* A32, 453-466.
 MOON, R. M., KOEHLER, W. C., CABLE, J. W. & CHILD, H. R. (1972). *Phys. Rev. (B)*, 5, 937-1016.
 SCHNEIDER, J. R. (1974). *J. Appl. Cryst.* 7, 541-546.
 ZACHARIASEN, W. H. (1945). *Theory of X-ray Diffraction in crystals*. New York: John Wiley.
 ZACHARIASEN, W. H. (1967). *Acta Cryst.* 23, 558-564.